Laser linewidth effects in quantum state discrimination by electromagnetically induced transparency

M. J. McDonnell, D. N. Stacey, and A. M. Steane
Centre for Quantum Computation, Department of Atomic and Laser Physics, Clarendon Laboratory, Parks Road, Oxford, OX1 3PU, England
(Received 13 February 2004; published 4 November 2004)

We discuss the use of electromagnetically modified absorption to achieve selective excitation in atoms: that is, the laser excitation of one transition while avoiding simultaneously exciting another transition whose frequency is the same as or close to that of the first. The selectivity which can be achieved in the presence of coherent population trapping (CPT) is limited by the decoherence rate of the dark state. We present exact analytical expressions for this effect, and also physical models and approximate expressions which give useful insights into the phenomena. When the laser frequencies are near-resonant with the single-photon atomic transitions, CPT is essential for achieving discrimination. When the laser frequencies are far detuned, the "bright" two-photon Raman resonance is important for achieving selective excitation, while the "dark" resonance (CPT) need not be. The application to laser cooling of a trapped atom is also discussed.

DOI: 10.1103/PhysRevA.70.053802 PACS number(s): 42.50.Gy, 32.80.Bx

Coherent population trapping [CPT, also called dark resonance or electromagnetically induced transparency (EIT)] and phenomena related to it have been widely studied (see for example [1,2] and references therein). These two-photon resonance phenomena can give rise to sharp spectral features, which can be used for various purposes, including for example magnetometry and laser cooling [3–8]. Recently, it was shown that CPT could be used to allow the angular momentum state of an atom to be detected with high quantum efficiency even in the absence of a Zeeman effect (i.e., at zero applied magnetic field and/or zero magnetic dipole moment of the atom) [9]. This paper develops the theory relevant to the latter, and sheds light on related experimental techniques such as laser cooling.

In an ion trap experiment the use of narrow two photon resonances and dark states can be used to enhance the sideband cooling rate to the trap ground state [7]. Another application of the techniques described in this paper lies in the field of quantum information processing. Closely separated Zeeman levels may be used to store a qubit of quantum information in an atomic system [10]. To read out the qubit state selective excitation from individual Zeeman levels is required. This can be enhanced by use of a narrow two-photon resonance, or by suppression of excitation on an unwanted transition using CPT [9].

The essential concept here is the use of a two-photon resonance to achieve selective excitation. We are concerned with two states, generally closely-spaced, which have allowed transitions separated in frequency by a small interval (or coincident in frequency). We denote these states by $|S\rangle$ and $|I\rangle$, for "suppressed" and "interacting" respectively. Let P_S, P_I be an experimentally observed signal, such as collected fluorescence, obtained when the atom is prepared in $|S\rangle$ or $|I\rangle$, respectively. We wish to irradiate the atom in such a way as to achieve a detectable signal P_I and maximise the ratio $r \equiv P_I / P_S$.

The states $|S\rangle$ and $|I\rangle$ could for example be magnetic substates of the same atomic energy level, or they could represent the same internal state, but different motional states of an atom, such as two vibrational states in a harmonic potential well. In the former case, a high value for r permits the atomic spin state to be detected [9]; in the latter, a high value for r implies that efficient laser cooling is possible [6,7,11,12].

Suppose the signal is collected fluorescence. Excitation out of a state $|S\rangle$ can sometimes be avoided by using light of appropriate polarization. For example, with circularly polarized light driving a transition $^2S_{1/2} - ^2P_{1/2}$, one of the $^2S_{1/2}$ magnetic sublevels does not couple to the radiation. This would allow $P_S \simeq 0$ (limited only by experimental precision). However, in such a case the population of $|I\rangle$ is rapidly moved by optical pumping to $|S\rangle$, and hence P_I is also small. Our interest here is in achieving high values of r without significant transfer of population between $|I\rangle$ and $|S\rangle$.

The basic idea of using CPT, and more generally a laser-induced modification of the optical response of the atom, is illustrated in Fig. 1. We consider two situations. In the case illustrated in Fig. 1(a), both $|S\rangle$ and $|I\rangle$ are connected by strong (e.g., electric-dipole allowed) transitions to upper states, such that the two transition frequencies are close together or even identical, but $|S\rangle$ is part of a three-level manifold D which can exhibit dark resonance, while $|I\rangle$ is not. An example of this is in a manifold $S_{1/2}, P_{3/2}, D_{3/2}$, with lasers of opposite circular polarization; the states $|I\rangle, |S\rangle$ are then sublevels of $S_{1/2}$ and level 2 is a stretched state of $D_{3/2}$. In the case illustrated in Fig. 1(b), both $|S\rangle$ and $|I\rangle$ are each part of separate three-level manifolds (called D and B for "dark" and "bright," respectively); both manifolds are driven simultaneously by a single pair of laser beams. An example of this is in a manifold $S_{1/2}, P_{3/2}, D_{3/2}$ again, but now with lasers of the same circular polarization.

Suppose the detected signal were the fluorescence from the atom. In either case (a) or (b), if the laser frequencies are chosen in such a way that the D manifold is at a dark resonance, but the B manifold is not, then in the limit of no decoherence of the dark state, the ratio $r \to \infty$. This is evident

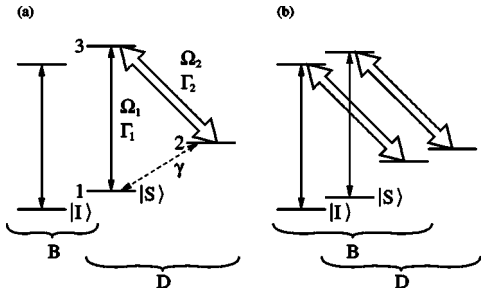

FIG. 1. Atomic level schemes considered in the text. (a) $|I\rangle$ is part of a two-level manifold; $|S\rangle$ is part of a three-level manifold. (b) $|I\rangle$ and $|S\rangle$ are each part of separate three-level manifolds. In either case, the atom is illuminated by a single pair of laser beams which drive both manifolds; the single photon transition 1-3 in the D manifold is either degenerate with or close to the single-photon transition out of $|I\rangle$ in the B manifold. Ω_1, Ω_2 are Rabi frequencies, Γ_1, Γ_2 spontaneous decay rates, and γ is the rate of decay of coherence between levels 2 and 1. Both types of energy level structure are common in groups of atomic levels with $J \neq 0$. Case (b) also occurs in the combination of internal and vibrational states of a trapped atom.

when the manifolds D and B are not connected, since then excitation from $|S\rangle$ will stop once the atom spontaneously enters the dark state, while excitation from $|I\rangle$ can continue indefinitely. It is also true when the upper state of manifold D can decay to $|I\rangle$ (which is more usual in practice), as long as we ensure an atom prepared in $|S\rangle$ remains dark as the laser beams are introduced. This can be done by introducing the "pump" laser, Rabi frequency Ω_2 in Fig. 1, first, and then switching on the "probe" laser of Rabi frequency Ω_1 adiabatically, i.e., on a time scale slow compared to the light shift caused by the pump laser.

In practice the available value of r is therefore limited by the loss of coherence of the dark state. For brevity we refer to this loss of coherence as a laser linewidth effect, although it can also be caused by other mechanisms. The laser linewidth is modeled as phase fluctuations in the pump and probe lasers producing homogeneous broadening of both. This is equivalent to elastic collisions producing phase fluctuations between the internal atomic states [13]. The effect on the dark state coherence is modeled simply as a decay rate γ of the off-diagonal density matrix element ρ_{21} in the optical Bloch equations for the D manifold. Note that many studies of phenomena related to CPT do not need to take this decoherence rate into account, except as a refinement, but here it is central. This model does not consider laser amplitude noise, time-of-flight broadening or inhomogeneous broadening. For specific applications it should not be difficult to extend the model to include these effects.

We wish to understand the selectivity r which can be achieved, as a function of all the relevant parameters. In order to do this, in Sec. I–V we model the atom as if the two manifolds B and D were not connected. If the excited state of D can in fact decay to B then such a model remains a good approximation as long as the population of the excited state of D is small. It will be seen that this is the case when $r \gg 1$. On the other hand, if the excited state of B can decay to D then the model does not apply. (In any case this situation would result in optical pumping from $|I\rangle$ to $|S\rangle$ and hence only a small signal P_I.) In the final Sec. VI concerning laser cooling, we allow a (small) nonzero branching ratio for either manifold to decay to the other.

The work was motivated by the idea that the phenomenon of dark resonance ought to make available especially high values of r. Our results show, however, that this is only partially true.

We assume the experimental signals P_S and P_I are proportional to the steady-state population of the excited state in the relevant manifold. This ignores a possible contribution from the initial transient behavior, for example during adiabatic switching on of the laser beams. The ignored contribution is negligible when the time scale on which the measured signal is obtained is long compared with the transient.

Our approach is to write down the steady state solution to the optical Bloch equations (OBEs) for a three-level atom excited by two laser fields of finite linewidth, and then examine the behavior of this solution. The full solution is a rather complicated function of many parameters. In previous work it has been obtained and then studied in a simplified form under various restrictions, such as low pump power or zero detuning. One of the aims of this paper is to provide analytical expressions which retain as great a range of validity as possible, while being sufficiently simple to give clear general insights into the physical behavior. This is done by finding factorizations of parts of the formulas, and by making good choices of the parameters with which to express them. We also present physical pictures to give further insight into the behavior.

We consider two regimes in detail: first the resonant case $\Delta_1 = \Delta_2 = 0$, and then the far-detuned case $\Delta_1 \gg \Gamma$ where $\Delta_1 = \omega_{L1} - \omega_{31}, \Delta_2 = \omega_{L2} - \omega_{32}$ are the detunings of the lasers from their respective single-photon transitions, and Γ is the width of the upper state.

The case of Fig. 1(a) is interesting because it permits a high degree of state discrimination even when the single-photon transitions from $|S\rangle$ and $|I\rangle$ have the same frequency. In this situation frequency discrimination of the bare single-photon transitions is ruled out completely, hence the CPT is crucial to achieving any discrimination. It was shown in Ref. [9] that this can be used to measure an atomic spin state at zero magnetic field or zero magnetic dipole moment. The choice $\Delta_1 = \Delta_2$ is used to make the dark resonance of the D system as dark as possible, while setting both detunings equal to zero causes the B system to give the maximum single-photon scattering rate. The value of r is derived in Sec. III; it is found to be proportional to the intensity of the pump laser in the D system, divided by γ.

In the case of Fig. 1(b), both manifolds D and B exhibit the phenomena of dark and bright 2-photon resonances. In order to obtain a good discrimination at finite laser linewidth, we require a frequency separation between the bright resonances of the two manifolds. This will occur either if there are suitable energy level separations in the atomic structure, or if the coupling strengths on the pump transitions are sufficiently different to cause a substantial difference in ac Stark shifts (light shifts) in the two manifolds. We discuss the case of Fig. 1(b) in detail because it is more complicated and the results are surprising. We find that although tuning the D

manifold to dark resonance does not do any harm (for the purpose of maximizing r), it does not permit any increase in the value of r compared to that available at large Δ_1, Δ_2, where the dark resonance disappears. Furthermore, the fact that the dark resonance causes one side of the Fano profile to fall substantially below a Lorentzian profile of the same height and width, which suggests that it would enhance discrimination, is misleading. It turns out that at given laser linewidth, the best choice of the other laser parameters is such that the width of the Fano profile is dominated by the laser linewidth, and in this situation it takes a Lorentzian form.

These conclusions apply when the decoherence of the dark state is caused by phase diffusion, leading to Lorenztian line shapes. When other noise sources dominate, such as laser drift or jitter with a non-Lorentzian profile, then the presence of a dark resonance can, in contrast, be useful.

In the context of laser cooling, the implication is that for given laser intensities and linewidths, the intrinsic lower limit on the steady-state temperature is always obtained at large detuning, where the bright resonance is important but the dark resonance (CPT) is not. However, sometimes a fast cooling rate is important, for example when further heating mechanisms are present, and then the dark resonance may be useful since it provides an increased cooling rate for a given temperature.

The paper is organized as follows. Section I briefly presents the case of frequency discrimination using single-photon excitation, in order to have a performance measure with which to compare our results. Section II presents the OBEs and their steady-state solution. Section III discusses the resonant case $\Delta_1 = \Delta_2 = 0$, and Sec. IV discusses the far-detuned case $\Delta_1 \gg \Gamma$. We simplify the equations and present two physical models which give useful insights into the bright resonance and its dependence on the laser parameters. Section V then discusses the discrimination which is available by using the bright resonance in the situation of Fig. 1(b). In Sec. VI the same ideas are applied to the case of laser cooling of a trapped atom or ion, by presenting numerical solutions of the master equation describing the evolution of both internal and motional states, in the Lamb-Dicke limit.

I. NARROW SINGLE-PHOTON TRANSITIONS

Before examining the 2-photon phenomena, we consider a simpler situation in order to obtain a "benchmark" with which to compare the performance. If there exist single-photon transitions out of the states $|S\rangle$ and $|I\rangle$ having different frequencies, then one could excite the atom with a single laser and simply use the different single-photon excitation rates which result when one transition is resonant and the other is not. To make a useful comparison, we need to consider a case where the discrimination available in such a method is limited by the laser linewidth γ_L rather than the natural (or other) linewidth of the transitions; we ignore also the possiblity of optical pumping. Then the excitation rate for either transition, as a function of laser frequency, is a Lorentzian function of FWHM γ_L. We tune the laser to resonance with the B manifold, and the system D is driven off-resonantly, with detuning Z given by the separation of the two transitions involved. For simplicity, we take the atom-laser coupling (electric dipole matrix elements) to be the same for the two transitions; then the ratio of excitation rates is

$$r = \frac{(\text{Excitation rate at } \delta = 0)}{(\text{Excitation rate at } \delta = Z)} \tag{1}$$

$$= \frac{Z^2 + (\Gamma'/2)^2 + \Omega^2/2}{(\Gamma'/2)^2 + \Omega^2/2} \tag{2}$$

$$\approx \left(\frac{2Z}{\gamma_L}\right)^2 + 1, \tag{3}$$

where δ is the detuning from resonance, $\Gamma' = \Gamma + \gamma_L, \Gamma \ll \gamma_L$ is the lifetime of the upper level, Ω is the Rabi frequency of the laser and it is assumed that the laser is not saturating the transition.

II. OPTICAL BLOCH EQUATIONS FOR 3-LEVEL ATOM

We adopt an interaction picture. Then in the rotating wave approximation (RWA), the OBEs for a 3-level Λ system with two lasers are (cf. [14,15])

$$\dot{\rho}_{33} = -\Gamma\rho_{33} - i(\rho_{13} - \rho_{31})\Omega_1/2 - i(\rho_{23} - \rho_{32})\Omega_2/2, \tag{4}$$

$$\dot{\rho}_{11} = \Gamma_1\rho_{33} + i(\rho_{13} - \rho_{31})\Omega_1/2, \tag{5}$$

$$\dot{\rho}_{22} = \Gamma_2\rho_{33} + i(\rho_{23} - \rho_{32})\Omega_2/2, \tag{6}$$

$$\dot{\rho}_{13} = (-\Gamma_{13} - i\Delta_1)\rho_{13} - i(\rho_{33} - \rho_{11})\Omega_1/2 + i\rho_{12}\Omega_2/2, \tag{7}$$

$$\dot{\rho}_{23} = (-\Gamma_{23} - i\Delta_2)\rho_{23} - i(\rho_{33} - \rho_{22})\Omega_2/2 + i\rho_{21}\Omega_1/2, \tag{8}$$

$$\dot{\rho}_{12} = i(\Delta_2 - \Delta_1)\rho_{12} + i\rho_{13}\Omega_2/2 - i\rho_{32}\Omega_1/2 - \gamma\rho_{12}, \tag{9}$$

where Ω_1 and Ω_2 are the Rabi frequencies of the "probe" and "pump" lasers exciting transitions 1-3 and 2-3, respectively, Γ is the decay rate of the upper state 3, Γ_1 and Γ_2 are the decay rates of 3 to 1 and 2, respectively (in a closed system, $\Gamma = \Gamma_1 + \Gamma_2$); the decay rates of the coherences are $\Gamma_{13}, \Gamma_{23}, \gamma \equiv \Gamma_{12}$. In the case where the coherence decay is purely associated with the finite lifetime of level 3, and with laser linewidths γ_1, γ_2, the coherence decay rates are given by

$$\Gamma_{13} = (\Gamma + \gamma_1)/2, \tag{10}$$

$$\Gamma_{23} = (\Gamma + \gamma_2)/2, \tag{11}$$

$$\gamma = (\gamma_1 + \gamma_2)/2. \tag{12}$$

The last equation, Eq. (12), applies when the two laser beams have independent dephasing, which is typically the case if they originate in different lasers. If they both originate in the same laser, with a frequency difference imposed by another device such as an acousto-optic modulator, then Eq. (12)

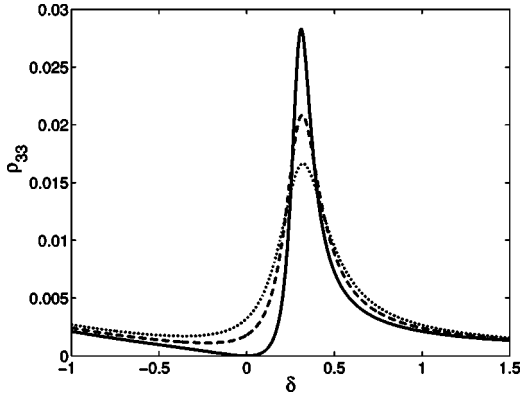

FIG. 2. Example fluorescence profiles for a set of values of laser linewidth. The parameter values are (in units where $\Gamma=1$) $\Omega_1=0.1$, $\Omega_2=1$, $\Delta_2=3$, $\Gamma_1=\Gamma_2=0.5$, and $\gamma=0$, 0.05, 0.1 for full, dashed, dotted curves, respectively. Note that at finite γ the absorption minimum is displaced with respect to $\delta=0$, as remarked by Kofman [16].

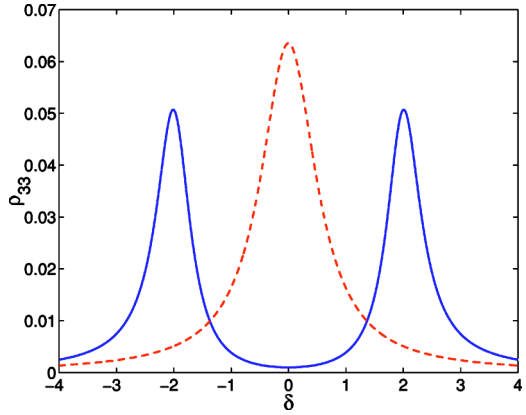

FIG. 3. Example of state discrimination for atomic structure of the form shown in Fig. 1(a). The curves show the steady-state value of the excited state population for an atom prepared in $|S\rangle$ (full curve) and $|I\rangle$ (dashed curve), respectively, as a function of detuning δ. The B manifold shows the standard "2-level atom" Lorentzian profile, while the D manifold shows a dark resonance at $\Delta_1=0$ in between two peaks at $\pm\Omega_2/2$ (these show the positions of the dressed states created by the pump laser). By choosing $\delta=0$ the ratio of excitation rates is maximized. The parameter values for the three level system are (in units where $\Gamma=1$) $\Omega_1=0.2$, $\Omega_2=4$, $\Gamma_1=\Gamma_2=0.5$, and $\gamma=0.1$. For the two level system $\Omega_1=0.2\sqrt{2}$ and $\Omega_2=0$.

does not apply and instead γ is equal to the rate of dephasing of the imposed frequency difference. In the rest of the paper, we will make the simplifying assumption $\Gamma_{23}=\Gamma_{13}$, so that both are equal to $\alpha\Gamma/2$. This is valid when the lasers linewidths are equal, and approximately valid when they are unequal but small compared to Γ.

Any one of Eqs. (4)–(6) can be replaced using the normalization condition

$$\rho_{11}+\rho_{22}+\rho_{33}=1 \tag{13}$$

in order to get a linearly independent set of equations. The general solution of Eqs. (4)–(13) in steady state is given in the Appendix .

We define a parameter $\alpha\equiv 2\Gamma_{13}/\Gamma$. The definition implies that $\alpha\simeq 1$ when $\gamma\ll\Gamma$. Then the steady state value of the upper state population is

$$\rho_{33}=2\Omega_1^2\Omega_2^2\frac{[2\alpha\Gamma(\delta^2+\gamma^2)+(\Omega_1^2+\Omega_2^2)\gamma]}{c_0+c_1\gamma+c_2\gamma^2}, \tag{14}$$

where $\delta=\Delta_1-\Delta_2$ is the detuning from the dark resonance condition, and the coefficients c_i in the denominator are given in the Appendix .

Example profiles of the 2-photon resonance, as described by Eq. (14), are shown in Fig. 2. This illustrates the change in shape of the resonance as γ increases.

Although it is useful to have the full expression (14), it is too unwieldy to yield simple insights into the behavior. We therefore examine it in two limiting cases.

III. RESONANT LASERS

In the situation shown in Fig. 1(a), and such that the lower and upper energy levels in the B manifold are degenerate with states 1 and 3 (respectively) in the D manifold, then in order to optimize the discrimination factor r we choose $\Delta_1=\Delta_2=0$. There is then a dark resonance in the D manifold, while the B manifold is at a maximum in the fluorescence rate. The absorption in the D manifold is not completely cancelled owing to a nonzero decoherence rate γ.

For both lasers on resonance with their respective transitions, a factor $(\Omega_1^2+\Omega_2^2+4\Gamma_{13}\gamma)$ cancels in the full expression (14) for the excited state population in the D manifold. The expression reduces to

$$\rho_{33}^D=\frac{2\gamma\Omega_1^2\Omega_2^2}{\Omega^2 Y+2\gamma(3\Omega_1^2\Omega_2^2+2\Gamma_{13}Y)}, \tag{15}$$

where $\Omega^2\equiv\Omega_1^2+\Omega_2^2$ and $Y\equiv\Gamma_2\Omega_1^2+\Gamma_1\Omega_2^2$.

Assuming the atom-laser coupling constants are such that the Rabi frequency in the B manifold is equal to $C\Omega_1$, where C is a constant (e.g., a Clebsch-Gordan coefficient), and that the excited state in B has the same total decay rate Γ as the excited state in D, then the excited state population for the (two level) B manifold is

$$\rho^B=\frac{1}{2+\Gamma^2/C^2\Omega_1^2}. \tag{16}$$

The ratio of steady-state populations is therefore

$$r=\frac{\rho^B}{\rho_{33}^D}=\frac{\Omega^2 Y+2\gamma(3\Omega_1^2\Omega_2^2+2\Gamma_{13}Y)}{2\gamma\Omega_2^2(2\Omega_1^2+\Gamma^2/C^2)}. \tag{17}$$

This result is valid without restriction—no assumptions have yet been made about the laser intensities or atomic parameters (except those implicit in a master equation treatment in RWA).

In the limit of low probe laser intensity compared to the pump laser intensity, i.e.,

$$\Omega_1^2 \ll \Omega_2^2, \quad \frac{\Gamma_1}{\Gamma_2}\Omega_2^2, \tag{18}$$

the ratio is

$$r \approx \frac{\Omega_2^2 \Gamma_1}{2\gamma(2\Omega_1^2 + \Gamma^2/C^2)} \tag{19}$$

$$\approx \begin{cases} \dfrac{\Omega_2^2 \Gamma_1 C^2}{2\gamma\Gamma^2}, & \Omega_1^2 \ll \Gamma^2, \\ \dfrac{\Omega_2^2 \Gamma_1}{4\gamma\Omega_1^2}, & \Omega_1^2 \gg \Gamma^2. \end{cases} \tag{20}$$

Hence a large enough pump laser intensity permits very good discrimination to be achieved.

Figure 3 shows the steady state populations in the excited state for the $|I\rangle$ and $|S\rangle$ systems with the pump laser at zero detuning $\Delta_2 = 0$, as a function of the probe laser detuning Δ_1. The example parameter values are chosen to illustrate a case where $|I\rangle$ and $|S\rangle$ are adjacent Zeeman sublevels in the atomic ground state at zero magnetic field, and the excited states decay primarily to the ground state. This has recently been implemented experimentally in order to read out the state of a quantum bit stored in the Zeeman levels of the ground state of a trapped ion [9].

In the case of a ladder system, i.e., when level 2 lies above level 3 in the D manifold, the results are as follows. The OBEs, Eqs. (4) and (6) are modified so that the spontaneous emission at rate Γ_2 is now from 2 to 3, not the other way around. The steady state solution at zero detuning is

$$\rho_{33} = \frac{2\gamma\Omega_1^2\Omega_2^2 + \Omega_1^2\Gamma_2(\Omega_1^2 + 4\Gamma_{23}\gamma)}{\Omega^2\tilde{Y} - \Gamma_2\Omega_1^2[3\Omega_2^2 + 2\Gamma_1(\Gamma_{23} - \Gamma_{13})] + 2\gamma[3\Omega_1^2\Omega_2^2 + 2\Gamma_{13}\tilde{Y} + 4\Gamma_2(\Gamma_{23} - \Gamma_{13})\Omega_1^2]}, \tag{21}$$

where $\tilde{Y} = 2\Gamma_2\Omega_1^2 + \Gamma_1\Omega_2^2 + 2\Gamma_1\Gamma_2\Gamma_{23}$. In the case where the coherence decay rates are purely due to spontaneous emission and laser linewidths, then for the ladder system, Eqs. (11) and (12) should be replaced by

$$\Gamma_{23} = (\Gamma + \Gamma_2 + \gamma_2)/2, \tag{22}$$

$$\gamma = (\Gamma_2 + \gamma_1 + \gamma_2)/2. \tag{23}$$

(In a closed system, $\Gamma = \Gamma_1$.) In the limit $\Omega_2^2 \gg \Omega_1^2$ expressions (15) and (21) are the same.

IV. WEAK PROBE, LARGE DETUNING

We next examine the behavior for a weak probe intensity and large detunings:

$$\Omega_1^2 \ll \frac{\Gamma_1}{\Gamma_2}\Omega_2^2, \Gamma_1\alpha\Gamma, \tag{24}$$

$$\Delta_1^2 \gg \alpha^2\Gamma^2, \delta^2. \tag{25}$$

Under the weak probe condition (24) alone (i.e., without any restriction on detunings), we obtain

$$c_0 \simeq 16\Omega_2^2\Gamma_1\left[\Delta_1^2(\delta - \Delta')^2 + \delta^2(\alpha\Gamma/2)^2 + \delta^2\Delta_2^2\frac{\Omega_1^2}{\Omega_2^2}\frac{\Gamma_2}{\Gamma_1} + \frac{\Omega_2^2\Omega_1^2}{16}\left(\frac{\Gamma_2}{\Gamma_1} + 2\right)\right], \tag{26}$$

$$c_1 \simeq 16\Omega_2^2\Gamma_1\left[\frac{\alpha\Gamma\Omega_2^2}{4} + \frac{\Omega_1^2}{2\alpha\Gamma\Gamma_1}(\Gamma_1\Delta_1^2 + \Gamma_2\Delta_2^2 + (\Gamma_1 + \Gamma_2)\Delta_1\Delta_2)\right], \tag{27}$$

$$c_2 \simeq 16\Omega_2^2\Gamma_1(\Delta_1^2 + \alpha^2\Gamma^2/4), \tag{28}$$

where

$$\Delta' \equiv \frac{\Omega_2^2}{4\Delta_1}. \tag{29}$$

When $\Delta_1 = \Delta_2$, then Δ' is the light shift of the states 2 (upwards when $\Delta_2 > 0$) and 3 (downwards when $\Delta_2 > 0$) caused by the pump laser.

If condition (25) applies, there is a further simplification of the expressions for c_i, and substituting them into Eq. (14) gives

$$\rho_{33} = \frac{\Omega_{\rm eff}^2\left(\alpha\left(\frac{\delta^2+\gamma^2}{2\Delta'^2}\right)R+\gamma\right)/2\Gamma_1}{(\delta-\Delta')^2+\left(\frac{\delta\Gamma}{2\Delta_1}\right)^2\left(\alpha^2+\frac{\Gamma_2}{\Gamma_1}\frac{\Omega_{\rm eff}^2}{R^2}\right)+\frac{\Omega_{\rm eff}^2}{4}\left(\frac{\Gamma_2}{\Gamma_1}+2\right)+\left(\alpha+\frac{\Omega_{\rm eff}^2}{R^2}\frac{\Gamma}{\alpha\Gamma_1}\right)R\gamma+\gamma^2}, \tag{30}$$

where

$$R \equiv \frac{\Omega_2^2}{4\Delta_1^2}\Gamma \tag{31}$$

is (when $\Delta_1 \simeq \Delta_2$) the scattering rate on the strongly driven transition 2-3 per unit population in 2, and

$$\Omega_{\rm eff} \equiv \frac{\Omega_2\Omega_1}{2\Delta_1} \tag{32}$$

is the effective Rabi frequency for Rabi oscillations on the Raman resonance between levels 1 and 2. The reason for introducing R and $\Omega_{\rm eff}$ is that they yield physical insights which will become apparent below.

Many previous treatments of this problem in the limit (24) have assumed the further condition $\Omega_2 \gg \Omega_1\Delta_1/\Gamma$, which may usefully be written $R \gg \Omega_{\rm eff}$. It will be important for some of the results to be discussed that we have not made this assumption. A nice feature is that we can find readily understandable physical pictures for this more general case.

The fact that we have not assumed $R \gg \Omega_{\rm eff}$ implies that our results remain valid at large Δ_1. For example, away from the 2-photon resonance, i.e., $|\delta| \gg |\Delta'|$, the terms proportional to δ^2 in Eq. (30) dominate, and the result is

$$\rho_{33} \to \frac{\Omega_1^2\Gamma/\Gamma_1}{4\Delta_1^2}. \tag{33}$$

This agrees with the prediction of the rate equations for the three-level system. It can be understood as the excited state population due to single-photon excitation from level 1 by the weaker laser, with the stronger laser playing the role of "repumper."

At small Δ_1, Δ_2 Eq. (30) remains fairly accurate for small laser linewidth, since the terms which were neglected under assumption (25) are primarily in c_1 and c_2, not c_0.

A. Zero laser linewidth

Let us consider the situation at zero laser linewidth, in order to obtain some physical insights. In this case, $\gamma=0$ and $\alpha=1$. Equation (30) simplifies to

$$\rho_{33} = \frac{\Omega_1^2\delta^2\Gamma/\Gamma_1}{4\Delta_1^2(\delta-\Delta')^2+\delta^2\Gamma^2+4\delta^2\Delta_1^2\frac{\Omega_1^2}{\Omega_2^2}\frac{\Gamma_2}{\Gamma_1}+\frac{\Omega_2^2\Omega_1^2}{4}\left(\frac{\Gamma_2}{\Gamma_1}+2\right)}. \tag{34}$$

(We present the equation in terms of Ω_2, Ω_1 and Δ_1 in order to facilitate comparison with previous work [14,17].) This has a zero at $\delta=0$ (the dark resonance) and a peak at $\delta \simeq \Delta'$ (the bright resonance). The precise location of the peak is discussed in [14].

The denominator of Eq. (34) can be simplified to good approximation by replacing the occurrences of δ^2 by Δ'^2 while retaining the $(\delta-\Delta')$ term. This is a good approximation because it is accurate when $\delta=\Delta'$, and away from this detuning, the first term in the denominator dominates when Δ_1 is large. This substitution gives the canonical "Fano" type of profile [18]:

$$\rho_{33} \simeq \frac{\Omega_{\rm eff}^2(\delta/\Delta')^2R/4\Gamma_1}{(\delta-\Delta')^2+R^2/4+\Omega_{\rm eff}^2\Gamma/2\Gamma_1}. \tag{35}$$

The width of the peak is now easy to extract. The values of δ at which ρ_{33} is half its maximum value are given by

$$(\delta-\Delta') \simeq \frac{f}{2}\left(\frac{f}{\Delta'}\pm 1\right), \tag{36}$$

where

$$f = \left(R^2+\Omega_{\rm eff}^2\frac{2\Gamma}{\Gamma_1}\right)^{1/2} \tag{37}$$

is the FWHM of the peak and to simplify the right-hand side (RHS) we used the condition $f \ll \Delta'$ [which follows from Eqs. (24) and (25)].

We next present some physical insights into the behavior.

1. Two models

The main features of ρ_{33} are the zero at dark resonance and the peak at the bright resonance.

As many authors have discussed [1,2], the zero is due to a cancellation between the two excitation routes when the

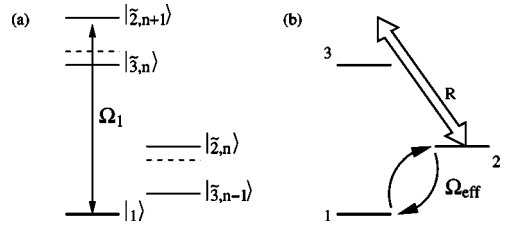

FIG. 4. Physical models of the bright resonance. (a) The pump laser dresses the atom; the probe laser excites the atom from $|1\rangle$ to the dressed states. These give a broad resonance displaced by $-\Delta'$ and a narrow resonance displaced by $\Delta_2+\Delta'$ from the position of the undressed excited state $|3\rangle$. (b) The two lasers together drive Rabi oscillations between (undressed) levels 1 and 2 by a Raman transition, and the pump laser off-resonantly excites transitions from $|2\rangle$ to $|3\rangle$. The Rabi oscillation is resonant when the laser frequencies match the energy difference between 1 and the Stark-shifted level 2.

atomic state is $(\Omega_2|1\rangle-\Omega_1|2\rangle)(\Omega_1^2+\Omega_2^2)^{-1/2}$ in an interaction picture. When $\delta=0$ this is a stationary state, so once in it the atom does not evolve out of it.

To understand the bright resonance, we present two physical models. The first is the well-known "dressed atom" approach; the second is an alternative model based on Rabi oscillations and the quantum Zeno effect. For general reviews and references on the quantum Zeno effect, see for example Refs. [19–22].

The application of the "dressed atom" treatment to CPT and related phenomena has been widely discussed; see [1,2] for an introduction and further references. In this model, the probe laser excites population from level 1 to a dressed state created by the intense pump laser [see Fig. 4(a)]. Near the centre of the bright resonance, i.e., when $\delta\simeq\Delta'$, Eq. (35) takes the form

$$\rho_{33}\simeq\frac{\Omega_{\rm eff}^2 R/4\Gamma_1}{(\delta-\Delta')^2+R^2/4+\Omega_{\rm eff}^2\Gamma/2\Gamma_1}. \tag{38}$$

Comparing this with the well-known expression for the upper state population of a two-level atom in steady state, we see that the result has a natural interpretation in the dressed atom model. The dressed state has decay rate R and the strength of the coupling to it is $\Omega_{\rm eff}$. The two terms which make up the FWHM (37) of the resonance are then to be interpreted as "natural linewidth" and "power broadening" of the dressed state.

Our alternative model is based on Rabi oscillations and the Zeno effect, as follows (cf. [23]).

When the difference frequency δ is tuned to the light shift Δ', the pump and probe lasers drive resonant Rabi oscillations between level 1 and the light-shifted level 2. Observe that when $\Omega_2\gg\Omega_1$ and neither of the single-photon transitions are saturated, the population ρ_{33} is produced primarily by excitation from level 2. The excited state population thus comes about from the combination of the Rabi oscillation which moves population between 1 and 2, and single-photon excitation from 2 to 3 [see Fig. 4(b)]. However, the single-photon excitation results in a spontaneously emitted photon when 3 decays, and therefore constitutes a measurement of the atom's state in the 1, 2 basis. This measurement suppresses the Rabi oscillations by the quantum Zeno effect. The steady state solution finds a balance between these effects.

This physical picture suggests the following analysis. We take the limit $\Omega_2\gg\Omega_1$ such that population in 3 is produced purely by excitation from 2 by the pump laser, and treat this by the rate equation

$$\dot{\rho}_{33}=R_2\rho_{22}-\Gamma\rho_{33}, \tag{39}$$

where the single-photon excitation rate R_2 is given by the Fermi golden rule: $R_2=(\pi/2)\Omega_2^2 g(\Delta_2)$ where g is a line shape function. Hence in steady state,

$$\rho_{33}=\frac{R_2\rho_{22}}{\Gamma}. \tag{40}$$

The spontaneous decay of ρ_{33} leads to a Lorentzian line shape of width Γ, so in the limit $\Delta_2\gg\Gamma,\Omega_2$,

$$R_2\simeq\frac{\Omega_2^2}{4\Delta_2^2}\Gamma. \tag{41}$$

We calculate the steady-state population ρ_{22} by considering the Rabi oscillations between levels 1 and 2, and taking ρ_{22} to be the mean population averaged over time. When R_2 is sufficiently small, and the Raman process is resonant, this Rabi oscillation leads to equal average populations ρ_{11} and ρ_{22}, i.e., both equal to $1/2$. When R_2 is non-negligible, on the other hand, the Rabi oscillation is interrupted by photon scattering events. These act like measurements, and suppress the oscillations by the Zeno effect when they are sufficiently frequent.

An uninterrupted Rabi oscillation process would cause the population ρ_{22} to vary with time as

$$\rho_{22}(t)=\frac{\Omega_{\rm eff}^2}{\delta'^2+\Omega_{\rm eff}^2}\sin^2\frac{1}{2}(\Omega_{\rm eff}^2+\delta'^2)^{1/2}t, \tag{42}$$

where $\delta'=\delta-\Delta'$ is the detuning from the Raman resonance (bright resonance), $\Omega_{\rm eff}$ is given in Eq. (32). The photon scattering acts both as a measurement-type process, collapsing the state to either 1 or 2, and also causes optical pumping to 1. We will treat a simplified case in which we assume the population always goes to 1 after photon scattering, and then the population in 2 recommences evolving as Eq. (42). This would be the behavior to be expected when $\Gamma_1\gg\Gamma_2$. In this case the mean population of 2 is estimated as

$$\overline{\rho}_{22}\simeq\int_0^\infty P(t)\rho_{22}(t)dt, \tag{43}$$

where $P(t)=R_2e^{-R_2t}$ is the probability that there is an interval t between scattering events. Performing the integral in Eq. (43) we obtain

$$\overline{\rho}_{22}\simeq\frac{1}{2}\frac{\Omega_{\rm eff}^2}{\delta'^2+R_2^2+\Omega_{\rm eff}^2} \tag{44}$$

and substituting this in Eq. (40) gives

$$\rho_{33} \simeq \frac{\Omega_{\rm eff}^2 R_2/2\Gamma}{\delta'^2 + R_2^2 + \Omega_{\rm eff}^2}. \tag{45}$$

Note the similarity between Eqs. (45) and (38). The Zeno effect calculation reproduces the OBE result when $\Gamma_1 \simeq \Gamma$, except for factors of 2 associated with R_2 and $\Omega_{\rm eff}^2$. This confirms that it gives a good physical insight into the behavior. Of course a full quantum Monte Carlo type of calculation [24,25] would reproduce the OBE result exactly. The present result simply demonstrates the validity of the "Rabi-oscillation/Zeno effect" physical picture.

2. Two regimes

The above insights allow us to identify two distinct regimes of behavior. When $R \gg \Omega_{\rm eff}$, the Zeno effect strongly suppresses the Rabi oscillations. In this "Zeno regime,"

$$\rho_{33}^{\max} = \frac{\Omega_{\rm eff}^2}{R\Gamma_1} = \frac{\Omega_1^2}{\Gamma_1\Gamma}, \quad W_{\rm FWHM} = R, \tag{46}$$

where $W_{\rm FWHM}$ is the full width at half maximum. The interpretation in the dressed state picture is that of weak excitation, such that the FWHM is equal to the dressed state's "natural linewidth" R.

When $R^2 \ll \Omega_{\rm eff}^2$ we obtain

$$\rho_{33}^{\max} = \frac{R}{2\Gamma}, \quad W_{\rm FWHM} = (2\Gamma/\Gamma_1)^{1/2}\Omega_{\rm eff}. \tag{47}$$

Here the Rabi oscillation leads to $\rho_{11} = \rho_{33} \simeq 1/2$, which leads directly to the value of $\rho_{33}^{\max}$, in particular the fact that it depends purely on R. The width of the resonance results from the detuning-dependence of the Rabi oscillation, and thus is governed purely by $\Omega_{\rm eff}$. In the dressed state picture this is the case where "power broadening" dominates.

B. Finite laser linewidth

We return to Eq. (30) in order to consider the effect of finite laser linewidth. A useful approximation is the same "trick" as was used for Eq. (35) where we replace the δ^2 in the denominator by Δ'^2. This considerably simplifies the denominator without much loss of accuracy:

$$\rho_{33} \simeq \frac{\Omega_{\rm eff}^2\left[\alpha\left(\frac{\delta^2+\gamma^2}{2\Delta'^2}\right)R + \gamma\right]/2\Gamma_1}{(\delta-\Delta')^2 + (\alpha R/2 + \gamma)^2 + \Omega_{\rm eff}^2(\Gamma/2\Gamma_1)(1 + 2\gamma/\alpha R)}. \tag{48}$$

Note that this result is similar to Eq. (35) with the substitution $R \to \alpha R + 2\gamma \simeq R + 2\gamma$. In other words, the main effect of finite laser linewidth is to increase the "linewidth" term in Eq. (35) by 2γ. In the Zeno picture this is an illustration of the fact that measurement-induced collapses have the same effect on a system as phase fluctuations. Their effects add to produce the overall linewidth.

1. Effect of laser linewidth on dark resonance

The conditions (24), (25) imply $\Omega_{\rm eff}^2 \ll \Delta'^2$. At $\delta = 0$, this can be used to simplify the denominator of Eq. (48). If we further assume

$$\gamma \ll \Omega_2^2/\Gamma \tag{49}$$

(which is not a severe constraint on the range of validity of the results) then we obtain

$$\rho_{33}^{\rm dark} \simeq \frac{\Omega_{\rm eff}^2\gamma/2\Gamma_1}{\Delta'^2 + \Omega_1^2\gamma/\alpha\Gamma_1 + \gamma^2} \tag{50}$$

$$= \frac{2\Omega_1^2\gamma/\Gamma_1}{\Omega_2^2 + (\Omega_{\rm eff}^2/R^2)(4\Gamma^2/\alpha\Gamma_1)\gamma + (4\Gamma/R)\gamma^2}. \tag{51}$$

This result can be interpreted as follows. The dark state is

$$|-\rangle = (\Omega_2|1\rangle - \Omega_1|2\rangle)(\Omega_1^2 + \Omega_2^2)^{-1/2}. \tag{52}$$

The combination of $|1\rangle$ and $|2\rangle$ that is orthogonal to this is

$$|+\rangle = (\Omega_1|1\rangle + \Omega_2|2\rangle)(\Omega_1^2 + \Omega_2^2)^{-1/2}. \tag{53}$$

Decoherence associated with finite laser linewidth evolves the state towards a random mixture of $|-\rangle$ with the state $|\sim\rangle$ given by

$$|\sim\rangle = (\Omega_2|1\rangle + \Omega_1|2\rangle)(\Omega_1^2 + \Omega_2^2)^{-1/2}. \tag{54}$$

A good insight is obtained by analysing the system in the orthonormal basis $\{|3\rangle, |-\rangle, |+\rangle\}$ (see Fig. 5). A complete master equation can be obtained in this basis [1]; that of course gives exactly the same predictions as those given by the OBEs in their standard form. However, it is noteworthy that the dependence of ρ_{33} on γ at the dark resonance point can be obtained to second order in γ by a rate equation approach, as follows.

The atom-laser interaction Hamiltonian is $H_I = \Omega_1|3\rangle\langle 1| + \Omega_2|3\rangle\langle 2|$, and the only nonzero matrix element of H_I in the chosen basis is $\langle 3|H_I|+\rangle = (\Omega_1^2 + \Omega_2^2)^{1/2}$. When $\Omega_2^2 \gg \Omega_1^2$, the spontaneous decay of $|3\rangle$ to $|-\rangle(|+\rangle)$ is at rate approximately $\Gamma_1(\Gamma_2)$ respectively, owing to the relative proportions of $|1\rangle$ and $|2\rangle$ in each of $|-\rangle$ and $|+\rangle$. We model phase decoherence by a spontaneous decay at the rate $\tilde{\Gamma}$ in both directions between $|-\rangle$ and $|+\rangle$. The rate is given by the decay rate $\gamma/2$ between $|-\rangle$ and $|\sim\rangle$, multiplied by the probability that an atom in $|\sim\rangle$ would be found in $|+\rangle$ if measured in the $|\pm\rangle$ basis:

$$\tilde{\Gamma} = \frac{\gamma}{2}|\langle - | + \rangle|^2 = \frac{2\gamma\Omega_1^2\Omega_2^2}{(\Omega_1^2+\Omega_2^2)^2} \simeq 2\gamma\Omega_1^2/\Omega_2^2. \quad (55)$$

Invoking the limit (25) to simplify the atom-light coupling term, the resulting set of rate equations is

$$\dot{\rho}_{33} = (\rho_{++} - \rho_{33})R - \Gamma\rho_{33}, \quad (56)$$

$$\dot{\rho}_{--} = \rho_{33}\Gamma_1 + (\rho_{++} - \rho_{--})\tilde{\Gamma}, \quad (57)$$

$$1 = \rho_{33} + \rho_{--} + \rho_{++}. \quad (58)$$

The solution is

$$\rho_{33} = \frac{R\tilde{\Gamma}}{R\Gamma_1 + 2(R+\Gamma)\tilde{\Gamma}} \quad (59)$$

$$\simeq \frac{2\Omega_1^2\gamma/\Gamma_1}{\Omega_2^2 + (\Omega_{\rm eff}^2/R^2)(4\Gamma^2/\Gamma_1)\gamma}, \quad (60)$$

where we have used $\tilde{\Gamma} \ll \Gamma_1$ which follows from Eq. (24). Equation (60) correctly reproduces all the features of Eq. (51) up to second order in γ. The essence of the dynamics when $\Gamma_1 \gg R \gg \tilde{\Gamma}$ is that population moves from 3 to the dark state at the rate Γ_1, and from the dark state to 3 (via $|+\rangle$) at the rate $\tilde{\Gamma}$.

Next we consider the overall shape of the 2-photon resonance. The range of values of δ which interests us is from 0 to approximately Δ', the position of the bright resonance. Examining Eq. (48) we find that when the laser linewidth is sufficient to produce the condition

$$\gamma \gg \alpha R \quad (61)$$

then the γ term in the numerator dominates the other terms. In this case there is no longer a local minimum near $\delta=0$; the dark resonance is completely "washed out." Therefore the condition (61) is sufficient to change the overall lineshape to one close to a Lorentzian function. Note that Eq. (61) always occurs at sufficiently large Δ_1, independent of the values of the other parameters.

In the case (61) and when also $\gamma \gg \Omega_{\rm eff}$, $\Omega_{\rm eff}^2/R$, the complete expression (30) becomes simply a Lorentzian function of linewidth γ, for $|\delta| \ll |\Delta'|$ [and for large $|\delta|$, see Eq. (33)].

2. Effect of laser linewidth on bright resonance

At the position of the bright resonance ($\delta=\Delta'$), the condition (49) is sufficient to make the γ^2 term in the numerator of Eq. (48) negligible. In this case Eq. (48) gives

$$\rho_{33}^{\rm bright} = \frac{(\Omega_{\rm eff}^2/2\Gamma_1)(\alpha R/2+\gamma)}{(\alpha R/2+\gamma)^2 + \frac{1}{2}\Omega_{\rm eff}^2(\Gamma/\Gamma_1)(1+2\gamma/\alpha R)}. \quad (62)$$

In the "Zeno regime" $\Omega_{\rm eff}^2 \ll R^2$ this leads to the simple result

$$\rho_{33}^{\rm bright} \to \frac{\Omega_{\rm eff}^2/2\Gamma_1}{\alpha R/2+\gamma}. \quad (63)$$

V. USING THE BRIGHT RESONANCE FOR SELECTIVE EXCITATION

We will now explore the use of the bright resonance as a sharp spectral feature, able to resolve two closely spaced transitions. We have in mind the situation where the atomic structure consists, to good approximation, of two Λ systems "side by side" as in Fig. 1(b). (Similar results can be expected for two ladder-systems.) Each of the levels 1, 2, 3 is split into two closely spaced components (such as Zeeman sublevels, or two rungs of a ladder of vibrational energy levels). We still have just two lasers, and we would like to drive one Λ-system without driving the other.

The system we want to drive is *B* and the system we would like not to drive is *D*. The measure of good discrimination to be adopted is the ratio *r* between the steady state value for ρ_{33} in the systems or manifolds *B* and *D*.

We will discuss the case where the two manifolds have the same coupling constants, so the same Rabi frequencies Ω_2, Ω_1, but different energy level spacings, such that when the Raman detuning is δ in system *B*, it is δ-*Z* in system *D*. The discrimination ratio is then

$$r = \frac{\rho_{33}(\delta)}{\rho_{33}(\delta - Z)}, \quad (64)$$

where $\rho_{33}(\delta)$ is given by Eq. (30). The effect of a difference in coupling constants between the two manifolds is outlined in the Appendix .

First consider the behavior at large detuning, $\Delta_1 \gg \Omega_1, \Omega_2, \gamma, \Gamma$, which we will refer to for brevity as "$\Delta_1 \to \infty$." Equation (30) gives

$$\rho_{33}(\Delta_1 \to \infty) = \frac{\Omega_{\rm eff}^2(2\alpha\Gamma(\delta^2+\gamma^2)/\Omega_2^2 + \gamma)/2\Gamma_1}{(\delta-\Delta')^2 + \gamma\Omega_1^2/\alpha\Gamma_1 + \gamma^2}. \quad (65)$$

At large Δ_1, the light shift is small compared to *Z*, so to produce the discrimination factor *r* the dark resonance is irrelevant. We tune system *B* to bright resonance, and it is found that *r* is maximized at low probe power, $\Omega_1^2 \ll \gamma\Gamma \ll \Omega_2^2$. In this case, using Eqs. (64) and (65),

$$r(\Delta_1 \to \infty) = \frac{Z^2+\gamma^2}{(2\alpha\Gamma Z^2/\Omega_2^2 + \gamma)\gamma}. \quad (66)$$

Next let us consider the case where we arrange that $\Delta' = Z$. This means that when the *B* system is tuned to bright resonance, the *D* system is simultaneously tuned to dark resonance, and we expect a large value for *r*. Examining the ratio $r = \rho_{33}^{\rm bright}/\rho_{33}^{\rm dark}$ given by Eqs. (62) and (50), it is found that *r* is maximized in the "Zeno regime" $\Omega_{\rm eff}^2 \ll R^2$. It is always possible to enter this regime without affecting the light shift by reducing Ω_1 at fixed values of Ω_2 and Δ_1. From Eqs. (50) and (63) we then obtain

$$r(\Delta' = Z) = \frac{Z^2+\gamma^2}{(\alpha R/2+\gamma)\gamma}. \quad (67)$$

To maximize *r*, one should reduce *R* as much as possible, subject to the constraint $\Delta' = Z$. This means that, for given *Z*, the value of *R* is limited by the available laser power: $R = 4Z^2\Gamma/\Omega_2^2$, so

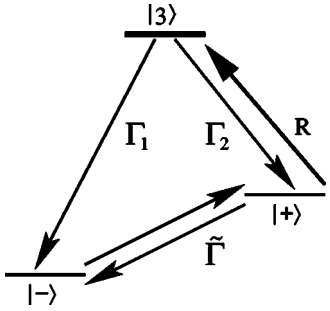

FIG. 5. Physical model of the effect of decoherence on a dark resonance. The atom is analyzed in the basis $|3\rangle,|+\rangle,|-\rangle$, where $|-\rangle$ is the dark state. A simple rate equation picture, with rates as shown, suffices to give the main features of the behavior.

$$r(\Delta' = Z) = \frac{Z^2 + \gamma^2}{(2\alpha\Gamma Z^2/\Omega_2^2 + \gamma)\gamma}. \tag{68}$$

This is the same result as Eq. (66). Therefore if Ω_1 is reduced sufficiently to enter the Zeno regime, then for laser linewidths satisfying $\gamma \ll \Omega_2^2/\Gamma$, the value of r is the same at $\Delta_1 = \Omega_2^2/4Z$ (where the D system is tuned to dark resonance) as when $\Delta_1 \to \infty$.

Discussion

The ratio $r = \rho_{33}(\delta)/\rho_{33}(\delta - Z)$ is plotted in Fig. 6 as a function of pump laser parameters Ω_2, Δ_2, for the example case of $Z = 0.2\Gamma$, $\gamma = 0.001\Gamma$, and small Ω_1. The ridge observed in the surface corresponds to the condition $\Delta' = Z$, with a slight offset owing to the displacement of the absorption minimum remarked in the caption to Fig. 2 (see below). Each line of r at constant Ω_2 has a local maximum at the ridge, and then tends to this same maximum r at large Δ_2. This is the basic behaviour predicted by Eqs. (66) and (68).

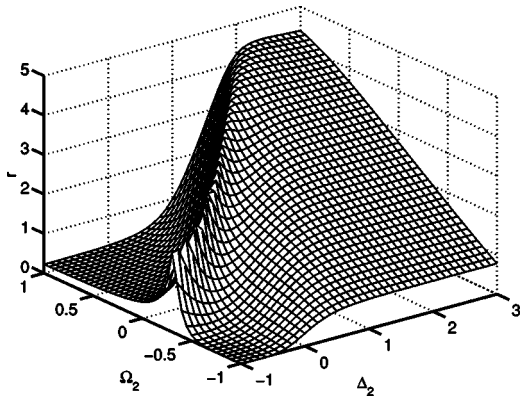

FIG. 6. Discrimination ratio r for the case of two Λ systems with the same coupling constants, and 2-photon resonance conditions of frequency separation Z. The surface shows r as a function of Δ_2 and Ω_2 for the case $Z = 0.2$, $\gamma = 0.001$, and small Ω_1, in units where $\Gamma = 1$. All scales are logarithmic, marked in powers of 10. Note that the range of validity of the approximate equation (30) is such that it gives the same results (i.e., no discernible difference in this surface plot) as the exact equation (14), even where Δ_1 is small.

A wider numerical exploration indicated that the value given by Eqs. (66) and (68) is always close to the maximum r when r is small enough to allow good discrimination ($r \gg 1$).

Equations (66) and (68) are among the central results of this paper. We had expected that arranging the special case where the light shift Δ' matches the offset Z would provide an especially good discrimination, as quantified by the ratio r. However, although we find that this case does provide the maximum r at given Z, γ and Ω_2, we find that the same value of r is also available when $\Delta' \neq Z$ by using a large detuning. Therefore the CPT can be useful to increase the rate of signal acquisition, but it does not provide an improved discrimination of the two resonances in the atom. Hence the title of this paper is a misnomer for the case considered here: the most important feature is the presence of the bright resonance, not the dark resonance. This could be called quantum state discrimination by "EIO", that is, electromagnetically-induced *opacity*.

At small Ω_2 and γ, r increases as Ω_2^2 and does not depend on Z, while at large Ω_2 it saturates to $r \to Z^2/\gamma^2 + 1$. The latter result is exactly the same as Eq. (3) for single-photon excitation limited by laser linewidth, if for given Z we compare the summed laser linewidths in the 2-photon case with the single laser linewidth in the single-photon case. This is owing to the Fano line shape becoming Lorentzian when the laser linewidth dominates its FWHM. The surprising feature is that choosing laser parameters in order to get a non-Lorentzian Fano profile, with its apparently useful sub-Lorentzian behavior near $\delta = 0$, in fact can only make matters worse at given laser linewidth and intensity.

Close inspection of the numerical results reveals a further detail. This is that for a strong pump beam, the optimal detuning is larger than that which leads to $\Delta' = Z$, and a slightly increased r is available. This is owing to the fact that for finite γ the minimum absorption is displaced from $\delta = 0$, as shown in Fig. 2. We find that this offset is given by $2\gamma\Delta_1/(\alpha\Gamma + 4\gamma)$, in agreement with [16]. An increase in Δ_1 reduces the light shift and hence allows the D manifold to be closer to the minimum when the B manifold is at the peak.

To summarize, in the case of two Λ-systems of the same coupling constant but different energy level separations, we find that the highest value of r is obtained both at $\Delta' = Z$, and at large Δ_2. Going to large Δ_2 has the disadvantage that the rates get small, so the system is more sensitive to drifts and other line-broadening mechanisms. Therefore the optimum conditions are, for given Z, γ:

$$\Omega_2 \text{ as large as possible}, \tag{69}$$

$$\Delta_2 = \frac{\Omega_2^2}{4Z}\left(1 + \frac{\gamma\Omega_2^2}{2\Gamma Z^2}\right) - Z, \tag{70}$$

$$\Omega_1 \ll \max\left(\frac{Z\Gamma}{\Omega_2}, \frac{\Delta\gamma}{\Omega_2}\right), \tag{71}$$

where in Eq. (70) we have included an adjustment for the displaced minimum, and the condition (71) is to avoid power-broadening of the bright resonance. Equation (68)

shows also that smaller laser linewidth is always advantageous to increase r, whereas r saturates as a function of Z, ceasing to increase significantly with Z once Z is large compared to $\Omega_2(\gamma/2\Gamma)^{1/2}$.

These conclusions are valid when the laser linewidth is caused by, or is equivalent to, phase diffusion. If other sources of noise, such as jitter and drift, dominate (with a non-Lorentzian frequency distribution) then the evaluation of r has to be reconsidered. In some circumstances it is appropriate to take average values of ρ_{33}^{dark} and $\rho_{33}^{\text{bright}}$, using Eqs. (62) and (50) averaged over the relevant laser frequency distribution. In certain cases the dark resonance can allow a much greater discrimination than would be obtained using narrow single-photon transitions driven by lasers with the same frequency distribution.

VI. LASER COOLING OF A TRAPPED ATOM

Laser cooling of a trapped 3-level atom using narrow two-photon resonances has been discussed by various authors (see Refs. [6,11] and references therein for a general discussion). We will examine the specific case of using the bright resonance (and accompanying dark resonance) for continuous cooling; this was considered by [6,7,11,12,26,27].

Using the formulation as given by [6], we obtain the steady state solution for the motional density matrix ρ_m of a trapped atom or ion in the Lamb-Dicke limit. Expanding the master equation to lowest order in the Lamb-Dicke parameters η_1, η_2 (associated with the laser excitation on transitions $1\leftrightarrow 3, 2\leftrightarrow 3$ respectively), the solution is found to be a thermal state $\rho_m=\Sigma(1-q)q^n|n\rangle\langle n|$ where $q=A_+/A_-$ is the ratio of heating- to cooling-rate coefficients. The rate coefficients $A_\pm$ are given by

$$A_\pm = (\Gamma_1\alpha_1\eta_1^2 + \Gamma_2\alpha_2\eta_2^2)\rho_{33} + \text{Re}\{\text{Tr}[2V(L_0 \pm i\nu)^{-1}V\rho]\}, \tag{72}$$

where α_1, α_2 are coefficients describing the angular distribution of spontaneously emitted photons (e.g., $\alpha=1/3$ for isotropic emission), ρ_{33} is the internal upper state population in steady state with motional effects ignored, i.e., as given by Eq. (14), V is the internal-state part of the laser-atom interaction which corresponds to first sideband excitation:

$$V = \eta_1\frac{\Omega_1}{2}(|3\rangle\langle 1| - |1\rangle\langle 3|) + \eta_2\frac{\Omega_2}{2}(|3\rangle\langle 2| - |2\rangle\langle 3|),$$

and L_0 is the zeroth order Liouville operator acting on the internal state, defined such that the master equation $\dot{\rho} = L_0(\rho)$ gives precisely the OBEs for the semiclassical treatment of a free atom, as given in Eqs. (4)–(9).

This situation may be compared with the selective excitation which is the main subject of this paper. Let ω_z be the vibrational frequency of the given atom in the (assumed harmonic) trap. Efficient cooling, and low steady-state temperature, is obtained when the cooling rate A_- is high and the heating rate A_+ is low. This requires strong excitation of the first red sideband at $\omega_0-\omega_z$ while avoiding excitation of the carrier and the first blue sideband, at ω_0 and $\omega_0+\omega_z$ respectively, where ω_0 is the centre of some resonance feature in the excitation spectrum of a free atom—in our case, the bright resonance. The energy level structure is akin to that of Fig. 1(b) rather than 1(a), since the ladder of vibrational energy levels leads to an infinite set of Λ systems. To obtain an enhancement from CPT, the lasers should be blue detuned, i.e., $\Delta_1, \Delta_2 > 0$. The frequency difference Z considered in Sec. V corresponds to the vibrational energy ω_z. The selectivity parameter r discussed in Sec. V corresponds to $1/q$. Just as we suspected that we might observe large selectivity r when $Z=\Delta'$, we now investigate whether we observe an especially low q when $\omega_z=\Delta'$.

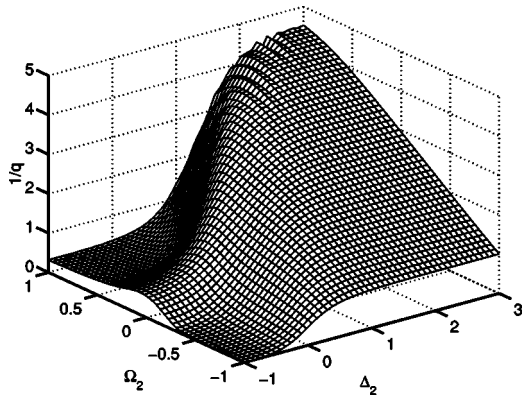

FIG. 7. Cooling/heating ratio $1/q$ for the case of laser cooling of a trapped three-level atom using the bright resonance. The surface shows $1/q$ as a function of Δ_2 and Ω_2 for the case $\omega_z=0.2, \gamma=0.001$, and small Ω_1, η_1, η_2, in units where $\Gamma=1$. All scales are logarithmic, marked in powers of 10. (The small irregular ripples at large $1/q$ are a numerical artifact.)

Figure 7 shows $1/q$ for the case of laser cooling, for the same parameters as were chosen in Fig. 6 for the case of r and selective excitation. The two sets of results are broadly similar. The main difference is that the ridge (i.e., high value of $1/q$, giving low temperature) produced by the "CPT condition" $\omega_z=\Delta'$ is now lower and broader, compared to the ridge in r in Fig. 6. This is because we now have many Λ systems, and the heating coefficient A_+ is produced both by the carrier and the blue sideband excitation: the dark resonance can suppress one or other of these, but not both. As a result, the lines of $1/q$ at constant Ω_2 show no local maximum as a function of Δ_2. q (and hence the steady-state temperature) falls monotonically as a function of pump laser detuning.

Although the CPT condition does not produce the lowest steady-state temperature T_0, for given values of pump laser intensity and trap frequency, it can be useful for other reasons. For example it was shown in [7] that it produces a high ratio A_-/T_0 of cooling rate to steady-state temperature, and permits cooling of motion in all directions to the same T_0.

ACKNOWLEDGMENTS

We thank Dr. Giovanna Morigi and Dr. Jürgen Eschner for helpful discussions on laser cooling using CPT, and Dr. David McGloin and Dr. David Lucas for comments on the manuscript. This work was supported by the EPSRC, ARDA

(P-43513-PH-QCO-02107-1), the Research Training and Development and Human Potential Programs of the European Union, and the Commonwealth Scholarship and Fellowship Plan.

APPENDIX

Here we present the solution of the OBEs for a 3-level Λ-type system.

The solution for ρ_{13} can be extracted by a standard matrix inversion method, see for example [2], where the case $\Delta_2 = 0$ is treated in full. We are interested here in ρ_{33} so we present this quantity.

The solution for $\gamma = 0$ has been presented by various authors, see for example [28] whose notation is close to ours. The solution for general γ was discussed in [6,29] and is closely related to the ladder system discussed in [15]. However the expressions in these works are even more lengthy and obscure than those given below; we require the simplest form possible.

In order to simplify the expressions without much loss of generality, we assume $\Gamma_{13} = \Gamma_{23}$ (this is valid when the lasers' linewidths are equal, and approximately valid when they are unequal but small compared to Γ).

In this case, the steady state value of ρ_{33} is as given in Eq. (14), with the coefficients in the denominator as follows:

$$c_0 = (\Omega_1^2 + \Omega_2^2)^2 Y + 16\delta^2\Gamma_{13}^2 Y + 4\delta^2\Omega_1^2\Omega_2^2[6\Gamma_{13} - (\Gamma_1 + \Gamma_2)] + 16\delta^2(\Gamma_2\Omega_1^2\Delta_2^2 + \Gamma_1\Omega_2^2\Delta_1^2) - 8\delta(\Delta_1\Gamma_1\Omega_2^4 - \Delta_2\Gamma_2\Omega_1^4), \tag{A1}$$

where $Y \equiv \Gamma_2\Omega_1^2 + \Gamma_1\Omega_2^2$,

$$c_1 = 2(\Omega_1^2 + \Omega_2^2)(4\Gamma_{13}Y + 3\Omega_1^2\Omega_2^2) + 4\frac{\Omega_1^2\Omega_2^2}{\Gamma_{13}}[\Gamma_1\Delta_1^2 + \Gamma_2\Delta_2^2 + (\Gamma_1 + \Gamma_2)\Delta_1\Delta_2] \tag{A2}$$

and

$$c_2 = 8[2\Gamma_{13}^2 Y + 3\Gamma_{13}\Omega_1^2\Omega_2^2 + 2(\Delta_2^2\Gamma_2\Omega_1^2 + \Delta_1^2\Gamma_1\Omega_2^2)]. \tag{A3}$$

Equation (A1) can also be written:

$$c_0 = 16\Omega_2^2\Gamma_1\Delta_1^2\left(\delta - \frac{\Omega_2^2}{4\Delta_1}\right)^2 + 16\Omega_1^2\Gamma_2\Delta_2^2\left(\delta - \frac{\Omega_1^2}{4\Delta_2}\right)^2 + 16\delta^2\Gamma_{13}^2 Y + 4\delta^2\Omega_1^2\Omega_2^2[6\Gamma_{13} - (\Gamma_1 + \Gamma_2)] + \Omega_1^2\Omega_2^2[Y + (\Omega_1^2 + \Omega_2^2)(\Gamma_1 + \Gamma_2)]. \tag{A4}$$

This form is useful in order to clarify where the resonances are, and to derive Eq. (26).

Degenerate Λ systems

Here we briefly discuss the case of two degenerate Λ systems, but where discrimination is still possible because of a difference in coupling constants.

We adapt the notation so that now the parameters Ω_i refer to manifold D, and we define $C_i = \Omega_i^B/\Omega_i$, $i = 1, 2$ where Ω_i^B are the Rabi frequencies in manifold B. The maximum r occurs either when system B is tuned to bright resonance, or when system D is tuned to dark resonance. The latter case is only relevant when γ is very small, and then r is a ratio of two very small excitation rates. We will concentrate on the case where γ is somewhat larger, and then it is best to tune B to bright resonance. We then have $r = \rho_{33}^B/\rho_{33}^D$ where ρ_{33}^B is given by Eq. (63):

$$\rho_{33}^B = \frac{C_1^2 C_2^2 \Omega_{\text{eff}}^2/2\Gamma_1 C_1^2}{\alpha C_2^2 R/2 + \gamma}. \tag{A5}$$

The symbols Ω_{eff}, R refer to their values in system D, and we assume the decay rate Γ_1 is enhanced in system B, compared to D, by C_1^2. We have also assumed the Zeno regime in order to avoid power broadening.

The situation in manifold D is given by Eq. (48) at $\delta = \Delta_B' - \Delta_D' = (C_2^2 - 1)\Delta'$, hence

$$\rho_{33}^D = \frac{\Omega_{\text{eff}}^2(\alpha R C_2^4/2 + \gamma)/2\Gamma_1}{(C_2^2 - 1)\Delta'^2 + (\alpha R/2 + \gamma)^2}, \tag{A6}$$

where we assumed Eq. (49). The largest values of r are obtained at high detuning, such that $R \ll \gamma$, where we find

$$r(\Delta_1 \to \infty) = [C_2(C_2 - 1)\Delta']^2/\gamma^2 + 1. \tag{A7}$$

[1] E. Arimondo, in *Progress in Optics*, edited by E. Wolf (North-Holland, Amsterdam, 1996), Vol. XXXV, pp. 257–354.
[2] M. O. Scully and M. S. Zubairy, *Quantum Optics* (Cambridge University Press, Cambridge, England, 1997).
[3] M. Fleischhauer and M. O. Scully, Phys. Rev. A **49**, 1973 (1994).
[4] M. Fleischhauer, T. McIllrath, and M. O. Scully, Appl. Phys. B: Lasers Opt. **60**, S123 (1995).
[5] A. Aspect, E. Arimondo, R. Kaiser, N. Vansteenkiste, and C. Cohen-Tannoudji, Phys. Rev. Lett. **61**, 826 (1988).
[6] M. Lindberg and J. Javanainen, J. Opt. Soc. Am. B **3**, 1008 (1986).
[7] G. Morigi, J. Eschner, and C. H. Keitel, Phys. Rev. Lett. **85**, 4458 (2000).
[8] J. Gea-Banacloche, Y-Q. Li, S-Z. Jin, and M. Xiao, Phys. Rev. A **51**, 576 (1995).
[9] M. McDonnell, J.-P. Stacey, S. C. Webster, J. P. Home, A. Ramos, D. M. Lucas, D. N. Stacey, and A. M. Steane, Phys. Rev. Lett. **93**, 153601 (2004).
[10] D. Stevens, J. Brochard, and A. M. Steane, Phys. Rev. A **58**, 2750 (1998).
[11] I. Marzoli, J. I. Cirac, R. Blatt, and P. Zoller, Phys. Rev. A **49**, 2771 (1994).
[12] D. Reiß, K. Abich, W. Neuhauser, Ch. Wunderlich, and P. E. Toschek, Phys. Rev. A **65**, 053401 (2002).
[13] R. Loudon, *The Quantum Theory of Light*, 3rd ed. (Oxford

University Press, New York, 2000).
[14] Y. Stalgies, I. Siemers, B. Appasamy, and P. E. Toschek, J. Opt. Soc. Am. B **15**, 2505 (1998).
[15] R. M. Whitley and C. R. Stroud, Jr., Phys. Rev. A **14**, 1498 (1976).
[16] A. G. Kofman, Phys. Rev. A **56**, 2280 (1997).
[17] D. Leibfried, R. Blatt, C. Monroe, and D. Wineland, Rev. Mod. Phys. **75**, 281 (2003).
[18] U. Fano, Phys. Rev. **124**, 1866 (1961).
[19] B. Misra and E. Sudershan, J. Math. Phys. **18**, 756 (1977).
[20] A. Beige and G. C. Hegerfeldt, Phys. Rev. A **53**, 53 (1996).
[21] W. L. Power and P. L. Knight, Phys. Rev. A **53**, 1052 (1996).
[22] B Misra and I Antoniou, in *Proceedings of the 22nd Solvay Conference on Physics: The Physics of Communication* (World Scientific, Singapore, 2003).
[23] F. B. de Jong, R. J. C. Spreeuw, and H. B. van Linden van den Heuvell, Phys. Rev. A **55**, 3918 (1997).
[24] J. Dalibard, Y. Castin, and K. Mølmer, Phys. Rev. Lett. **68**, 580 (1992).
[25] M. B. Plenio and P. L. Knight, Rev. Mod. Phys. **70**, 101 (1998).
[26] D. Reiß, A. Lindner, and R. Blatt, Phys. Rev. A **54**, 5133 (1996).
[27] G. Morigi, Phys. Rev. A **67**, 033402 (2003).
[28] G. Janik, W. Nagourney, and H. Dehmelt, J. Opt. Soc. Am. B **2**, 1251 (1985).
[29] R. G. Brewer and E. L. Hahn, Phys. Rev. A **11**, 1641 (1975).